Preliminary Seismic Hazard Model for South America

Mark Petersen, Steve Harmsen, Kathy Haller, Chuck Mueller, Nicolas Luco, Gavin Hayes, Jim Dewey, and Ken Rukstales

U.S. Geological Survey, Golden, CO

Introduction

The Centro Regional Sismological para América del Sur (CERESIS), U.S. Geological Survey (USGS), and Global Earthquake Model (GEM) organizations are collaborating to develop a new South America seismic hazard assessment (SASHA). CERESIS, the Regional Center for Seismology for South America, is an international organization created and supported by the governments of the South American countries, under a Multinational Agreement, ratified by law in each country that is interested in earthquake hazards and monitoring across the continent. The USGS has been involved for many years in reporting seismic events, conducting earthquake research, and assessing earthquake hazard across the globe for several decades. GEM is a new private/public organization that aims to be the uniform, independent standard to calculate and communicate earthquake risk worldwide. Each of these groups has interest in standardizing the hazard methodologies and data that pertain to hazard analysis. In this paper we describe the initial efforts of this group to develop hazard maps that can be applied to building codes and risk assessments.

The USGS has developed a preliminary seismic hazard model using available seismic catalogs, fault databases, and hazard methodologies to help facilitate discussions and to ascertain data requirements and availability. This preliminary seismic hazard model follows the methodology that was developed by the USGS for the United States (Petersen et al., 2008). The SASHA source model includes a smoothed seismicity component applied across the entire continent that accounts for earthquakes M 5-7, subduction zone sources M 7-9.5, and crustal faults M 7-8. The primary tectonics for this region involve subduction of the Nazca plate beneath

the west portion of the South American plate with related interface and intra-slab earthquakes and shallow crustal earthquakes.

South America Earthquake Catalog

We compiled a new catalog of instrumentally recorded earthquakes by combining four published global catalogs: (1) the IASPEI Centennial catalog compiled by Engdahl and Villaseñor (EVC; 2002); (2) the catalog originally compiled by Engdahl, van der Hilst, and Buland (EHB; 1998), and updated by Engdahl (personal communication); (3) the USGS/NEIC Preliminary Determination of Epicenters (PDE) on-line catalog (*http://neic.usgs.gov*); and (4) the International Seismological Centre (ISC) on-line catalog (*http://www.isc.ac.uk*). The combined catalog covers the years from 1900 to 2008 and the area from longitude 87° W to 32° W and latitude 58° S to 16° N. A single magnitude is selected for each earthquake from either the: (1) reported moment magnitude (M_w), (2) 20-second surface-wave magnitude (M_s), (3) the short-period P-wave magnitude (m_b), or (4) another magnitude, in that order of preference. Magnitudes are converted to moment magnitude (when possible) using relations published by Utsu (2002) and Sipkin (2003).

A basic assumption in the seismic hazard methodology is that earthquake sources are independent. Thus, catalogs that are used to estimate future seismic activity must be declustered (made free of dependent events such as foreshocks and aftershocks). We apply the declustering procedure of Gardner and Knopoff (1974) to eliminate foreshocks and aftershocks from the catalog. Gardner and Knopoff identified durations, T, and dimensions, L, as functions of mainshock magnitude, M, for a set of California data, and fit least-upper-bound envelopes to the data of the form: log T or log L = a M+ b, where a and b are regression parameters that quantify the rate and slope of the function. Following each earthquake in the chronologically ordered catalog, we scan for events within a [T(M),L(M)] window. If an event with magnitude less than or equal to M is found, it is deleted as an aftershock. For example, after a magnitude 6.0 earthquake, any smaller earthquake within 510 days and a radius of 54 kilometers is deleted. If an event with magnitude greater than M is found, the original earthquake is deleted as a foreshock.

To compute seismic hazard from seismicity we draw a sub-catalog from the declustered catalog based on earthquake depths and magnitude-completeness levels: depth less than or equal to 150 km; M_w greater than or equal to 5 since 1964 or M_w greater than or equal to 6 since 1900. This catalog contains 3312 earthquake records, with 805 contributed by EVC, 1450 by EHB, 686 by PDE, and 371 by ISC.

We separated the seismicity into shallow (less than 50 km depth), intermediate (greater than 50 km but less than 100 km depth), and deep (greater than 100 km but less than 150 km depth) earthquakes. Earthquakes deeper than 150 km are not considered in the model but should be added to future models.

Subduction Zone

The subduction zone geometry that is applied in this preliminary SASHA is based on new non-planar representations of the three-dimensional geometry of subducting slabs, incorporating data from historic seismicity and moment tensor catalogs, active source seismic surveys, regional aftershock deployment studies, and on the ridges and plate boundaries defined by published tectonic models (Hayes et al., 2009). Structural contours to 150 km depth are shown in Figure 1 and illustrate the variable dip of the plate interface.

Historical seismicity was used to define the recurrence parameters of the magnitude-frequency distributions defined for the sources. Figure 2 shows the zones, based on geomorphic and historic seismicity ruptures, that we define for analyzing seismicity statistics. Zones 1 through 5 represent areas associated with the upper 50 km of the subducting slab. All five zones have experienced earthquakes above M 8.0. Figure 3 shows a graph of earthquakes during the past 110 years as a function of magnitude. Zones 2 and 4 have the highest rate of earthquakes. Zone 5 hosted the 1960 M 9.5 Chile earthquake. We allow for M 7.0 to 9.5 in the two southern zones and M 7.0 to 9.0 in the northern three zones.

Crustal faults

We include a seismogenic source model for crustal faults to extend the instrumental seismic record. To model a seismogenic source, one must be able to define a generalized three-dimensional representation of the fault plane in the earth's crust and its mean activity rate. Strain rates in South America vary dramatically across the continent. Plate-boundary conditions prevail adjacent to the Caribbean, Pacific, and Antarctic coastlines where strain rates are high, similar to the western coast of North America. In contrast, the vast regions of the interior and the eastern part of the continent are considered relatively stable; however, historical global analogs show us that large earthquakes can occur in all of the represented geologic settings. Costa et al. (2006) provide an excellent overview of the tectonic environment and Quaternary deformation in South America.

This model includes crustal faults that have generated surface-faulting earthquakes in the geologically recent past and that may be capable of producing future, potentially damaging earthquakes. The input values are derived from summaries provided by well-informed experts with strong local or regional knowledge developed as part of the International Lithosphere Program's "World Map of Major Active Faults" and the International Decade for Natural Hazard Disaster Reduction. The USGS guided the effort to synthesize current geologic knowledge regarding Quaternary faults in South America that resulted in a series of digital maps and descriptions of Quaternary faults and folds (Audemard et al. 2000; Costa et al. 2000; Lavenu et al. 2000; París et al. 2000; Saadi et al. 2002; Eguez et al. 2003; Macharé et al. 2003).

Review of the various country compilations provide sufficient constraint to include 100 of the 350 known or suspected Quaternary faults recognized in South America. These faults are shown in Figure 4. Similar to the United States model, significantly less than one half of the known Quaternary faults have sufficient data to characterize its geometry and activity rate. With the exception of historic ruptures in South America, details of significant earthquakes on Quaternary faults are poorly constrained, and slip rate, a required input, is similarly unconstrained. Many of the faults in the continent are poorly studied and compilers did not assign a slip rate to nearly 80 percent. Over half of the remaining faults, were not included in this model because they are very short and the calculated M_{max} is less than M6.5. The 250 faults not included in this model generally are the oldest (defined as Quaternary in the compilations) and

slowest (<0.2 mm/yr) faults, which contribute little to hazard. Additional detailed investigations of the many potential sources in South America will improve future seismic hazard estimates.

Ground motion models

We apply the same ground motion prediction equations (GMPEs) for subduction interface and intraslab earthquakes, crustal earthquakes on faults in active tectonic regions, as well as crustal earthquakes on faults in cratonic and extended margin regions as those in corresponding tectonic regions in the US (Petersen et al., 2008). These GMPEs and their relative weights are discussed in the USGS National Seismic Hazard map update (Petersen et al., 2008). For subduction GMPEs, we have compared the models with data at distances from 100 to 1000 km and found that two GMPEs significantly over-predict the motion compared to global broadband data. Figure 5 shows the ground motion models applied for subduction zones. We have modified two of the three subduction GMPEs, Atkinson-Boore (2003), or AB03, and Youngs *et al.* (1997), or Geomatrix, to better fit these GDSN data. The Zhao *et al*. (2006) model was not revised, because GDSN data tended to be less at variance with their model.

Results

The seismic hazard map for peak ground acceleration having a 2% probability of exceedance in 50 years is shown in Figure 6. This is the hazard level that is applied in building codes for the U.S. Ground motions are highest near the subducting slabs along the western and northern coastlines of South America. Ground motions may also reach 0.1 to 0.3 g in many local areas across eastern South America. Disaggregation plots show the relative contribution to the hazard and have been produced for several major metropolitan areas. Figure 7 shows an example of one of these plots, in this case for 1-s spectral acceleration at a hazard level of 2% probability of exceedance in 50 years. This plot shows that for 1-s spectral acceleration local crustal faults may result in M ~ 7 earthquakes located within 50 km and contribute most to the hazard. However, there is also a smaller contribution from large M~9 subduction zone earthquakes located about 300 km away. Further analysis of these disaggregation plots will help engineers

recognize the most hazardous geologic faults and define the range of ground motions that could impact the site.

This analysis is a first cut at developing the input catalogs and source parameters needed to develop a South America Seismic Hazard Assessment. Many of these inputs should be improved with additional analysis. This effort will allow improvement of building code assessments, risk mitigation efforts, and public policy decisions.

References

Atkinson, G.M., and Boore, D.M., 2003, Empirical groundmotion relations for subduction-zone earthquakes and their application to Cascadia and other regions: Bulletin of the Seismological Society of America, v. 93, p. 1703–1729.

Audemard, F.A., Machette, M.N., Cox, J.W., Dart, R.L., and Haller, K.M., 2000, Map and database of Quaternary faults in Venezuela and its offshore regions: U.S. Geological Survey Open-File Report 00-018, 82 p.

Costa, C., Audemard, F.A., Bezerra, F.H.R., Lavenu, A., Machette, M.N., París, G., 2006, An overview of the main Quaternary deformation of South America: Revista de la Asociación Geológica Argentina, v. 61, no. 4, p. 461–479.

Costa, C., Machette, M.N., Dart, R.L., Bastias, H.E., Paredes, J.D., Perucca, L.P., Tello, G.E., and Haller, K.M., 2000, Map and database of Quaternary faults and folds in Argentina: U.S. Geological Survey Open-File Report 00-0108, 81 p.

Eguez, A., Alvarado, A., Yepes, H., Machette, M.N., Costa, C., and Dart, R.L., 2003, Database and map of Quaternary faults and folds of Ecuador and its offshore regions: U.S. Geological Survey Open-File Report 03-289, 77 p.

Engdahl, E.R., van der Hilst, R., and Buland, R., 1998, Global teleseismic earthquake location with improved travel-times and procedures for depth determination, Bulletin of the Seismological Society of America, v.88, 722–743.

Engdahl, E. R., and A. Villaseñor, 2002, Global seismicity — 1900-1999, *in* W.H.K. Lee, H. Kanamori, P.C. Jennings, C. and Kisslinger (editors), *International Handbook of Earthquake and Engineering Seismology*, Amsterdam, Academic Press, 665–690.

Gardner, J.K., and L. Knopoff L., 1974, Is the sequence of earthquakes in southern California, with aftershocks removed, Poissonian?: Bulletin of the Seismological Society of America, v.64, 1363–1367.

Hayes, G.P., Wald, D.J., and Keranen, K., 2009. Advancing techniques to constrain the geometry of the seismic rupture plane on subduction interfaces *a priori* – higher order functional fits, *Geochem. Geophys. Geosys., 10, Q09006.*

Lavenu, Alain, Thiele, Ricardo, Machette, M.N., Dart, R.L., Bradley, L-A., and Haller, K.M., 2000, Maps and database of Quaternary faults in Bolivia and Chile: U.S. Geological Survey Open-File Report 00-283, 50 p.

Macharé, J., Fenton, C.H., Machette, M.N., Lavenu, A., Costa, C., and Dart, R.L., 2003, Database and map of Quaternary faults and folds in Perú and its offshore region: U.S. Geological Survey Open-File Report 03-451, 55 p.

París, Gabriel, Machette, M.N., Dart, R.L.,and Haller, K.M., 2000 , Map and database of Quaternary faults and folds in Colombia and its offshore regions: U.S. Geological Survey Open-File Report 00-0284, 66 p.

Petersen, M.D., A.D. Frankel, S.C. Harmsen, C.S. Mueller, K.M. Haller, R.L. Wheeler, R.L. Wesson, Y. Zeng, O.S. Boyd, D.M. Perkins, N. Luco, E.H. Field, C.J. Wills, and K.S. Rukstales , 2008, Documentation for the 2008 update of the United States National Seismic Hazard Maps, U.S. Geological Survey, Open-file report 2008-1128, 60 pp., 11 appendices.

Saadi, Allaoua, Machette, M.N., Haller, K.M., Dart, R.L., Bradley, L-A., and de Souza, A.M.P.D., 2002, Map and database of Quaternary faults and lineaments in Brazil: U.S. Geological Survey Open-File Report 02-230, 63 p.

Sipkin, S.A., 2003, A correction to body-wave magnitude m_b based on moment magnitude M_w, Seismological Research Letters, 74(6), 739–742.

Utsu, T., 2002, Relationships between magnitude scales, *in* W.H.K. Lee, H. Kanamori, P.C. Jennings, and C. Kisslinger (editors), *International Handbook of Earthquake and Engineering Seismology*, Amsterdam, Academic Press, 733–746.

Youngs, R.R., Chiou, S.J., Silva, W.J., and Humphrey, J.R., 1997, Strong ground motion attenuation relationships for subduction zone earthquakes: Seismological Research Letters, v. 68, p. 58–73.

Zhao J.X., Zhang, J., Asano, A., Ohno, Y., Oouchi, T., Takahashi, T., Ogawa, H., Irikura, K., Thio, H., Somerville, P., Fukushima, Y., and Fukushima, Y., 2006 Attenuation relations of strong ground motion in Japan using site classification based on predominant period: Bulletin of the Seismological Society of America, v. 96, p. 898–913.

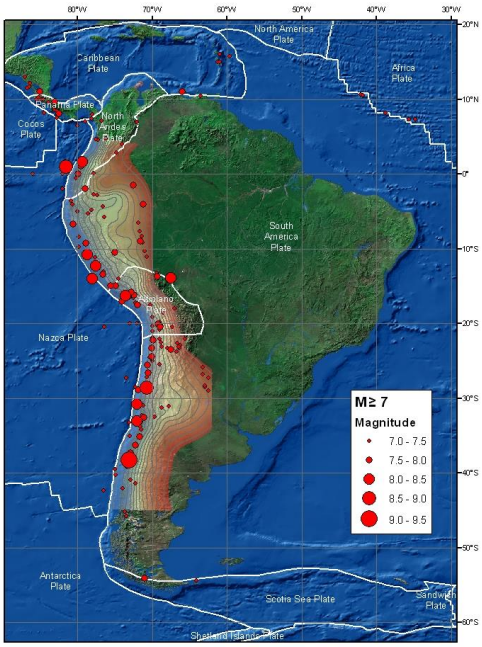

Figure 1. Preliminary model for active crustal tectonics in South America. Showing contours of the subducting slab depth (contour interval is 20 km), and earthquakes M>=7 since 1900 from the catalog.

Figure 2. Zones used for calculating seismicity statistics

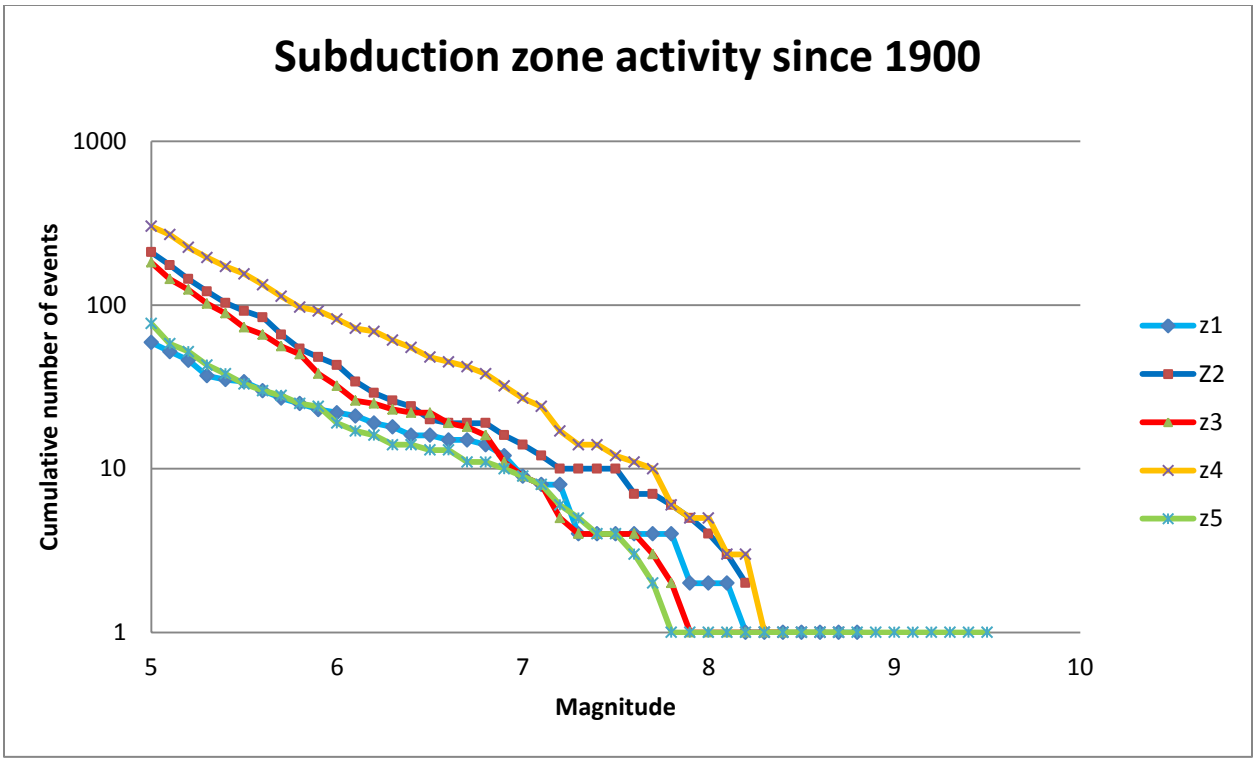

Figure 3. Earthquake statistics for zones 1-5 since 1900.

Figure 4. Crustal faults applied in hazard model.

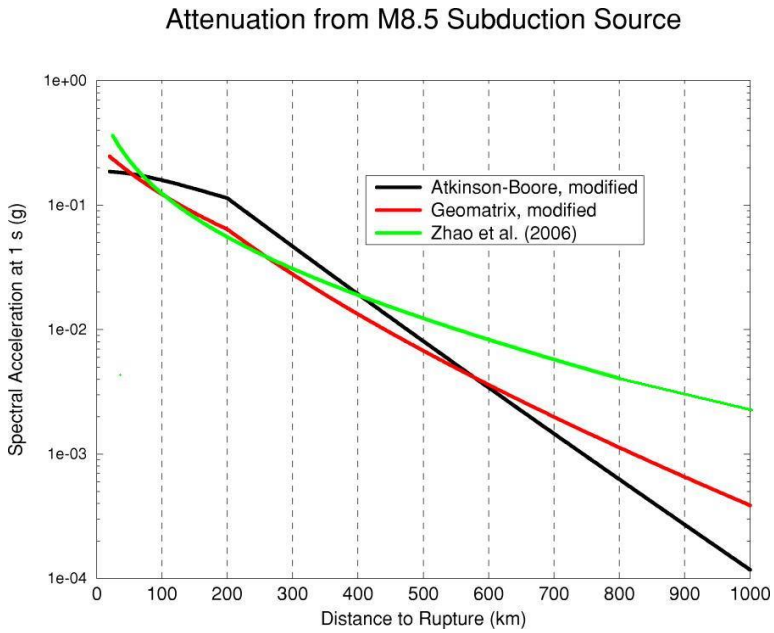

Figure 5. Plot showing ground motion prediction equations for subduction zone earthquakes for 1 second spectral acceleration at distances (Rcd) between 0 and 500 km. References for each of the curves can be found in Petersen et al., 2008.

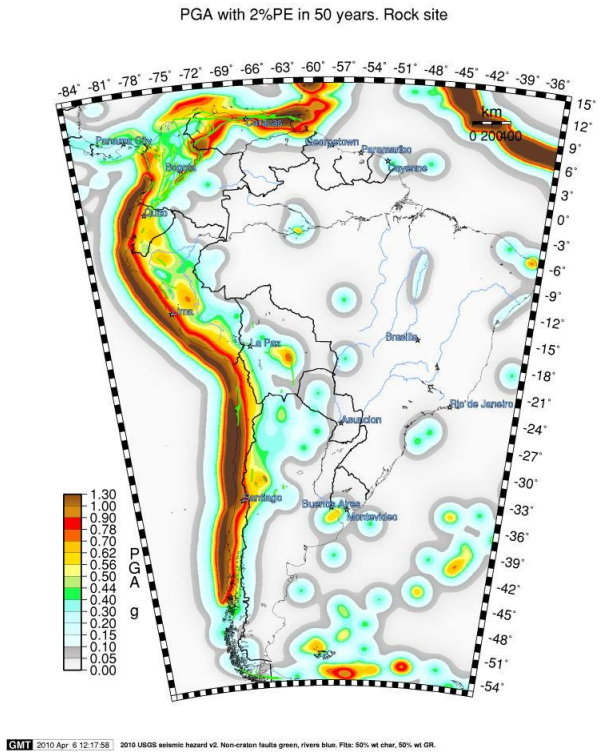

Figure 6. Preliminary peak horizontal ground acceleration seismic hazard map for South America for 2% probability of exceedance in 50 years on firm rock (760 m/s average shear wave velocity in upper 30 m).

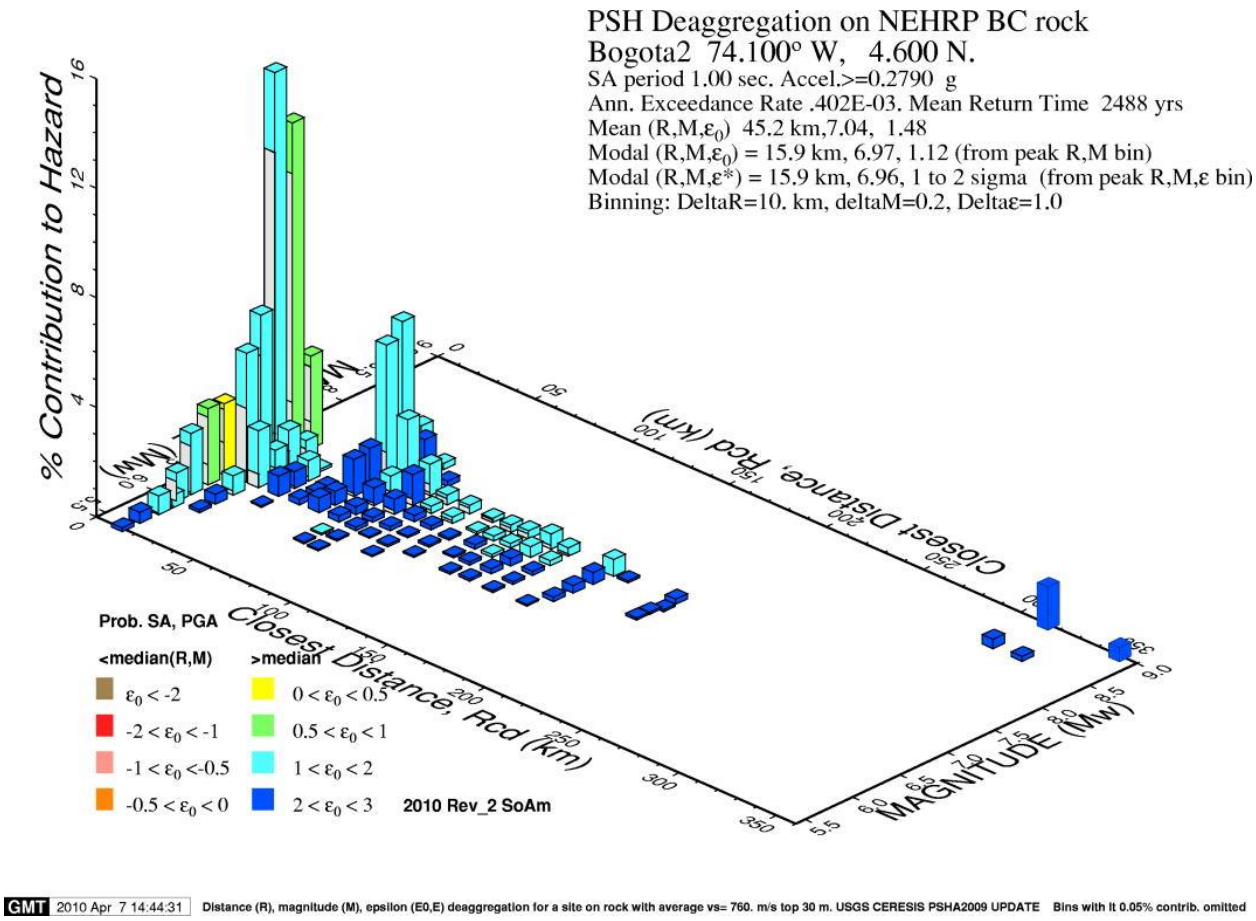

Figure 7. Disaggregation (also known as deaggregation) plot for Bogotá, Colombia. Plot shows that local crustal faults and subduction zone earthquakes are important to the hazard at a spectral acceleration of 1 second period and a return period of 1 in 2482 years (approximately 2% probability of exceedance in 50 years). The primary seismic hazard in this example is from earthquakes on the Afiladores fault, which contribute 45% of the total hazard at this site.